Supporting Information

Rapid SERS quantification of trace fentanyl laced in recreational drugs with portable Raman module

Hao Wang, [a‡] Zhaolin Xue, [a‡] Yuxuan Wu, [b] John Gilmore, [c] Lu Wang, [b] and Laura Fabris [a]*

a. Department of Materials Science and Engineering, Rutgers university, 607 Taylor Road, Piscataway, NJ, 08854 USA
b. Department of Chemistry and Chemical Biology, Rutgers university, 123 Bevier Road, Piscataway, NJ, 08854 USA
c. Hamamatsu Corporation, 360 Foothill Road, Bridgewater, NJ, 08807 USA

*E-mail: lfabris@soe.rutgers.edu (L. F.)

Table of Contents

a) TEM image of AgNPs   b) Zeta potential   c) UV-Vis absorption   d) Optical image
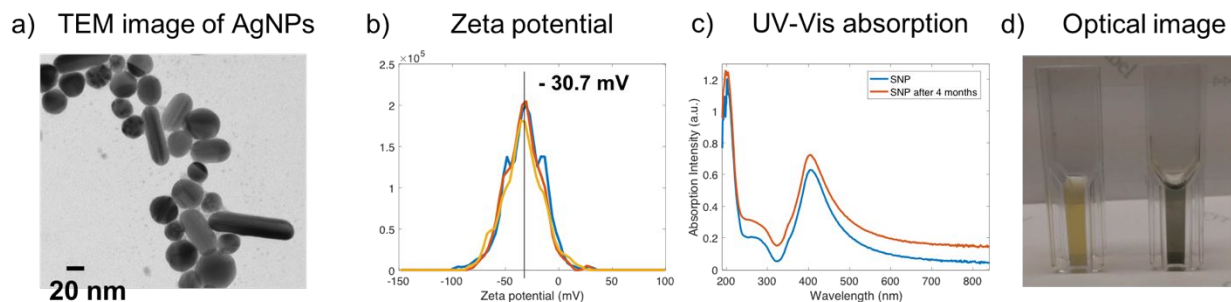
Figure S1: Physicochemical characterizations of the synthesized AgNPs. a) TEM image of as-synthesized Lee-Meisel AgNPs; b) zeta-potential measurements of the synthesized AgNPs; c) UV-Vis extinction profiles of AgNPs before SERS measurement (blue curve) and AgNPs after 4 months of storage (red curve); d) Optical images of 1 mL AgNP colloids with no salt addition (left) and 30 min after salt addition (right, 50 μL, 2M NaBr).
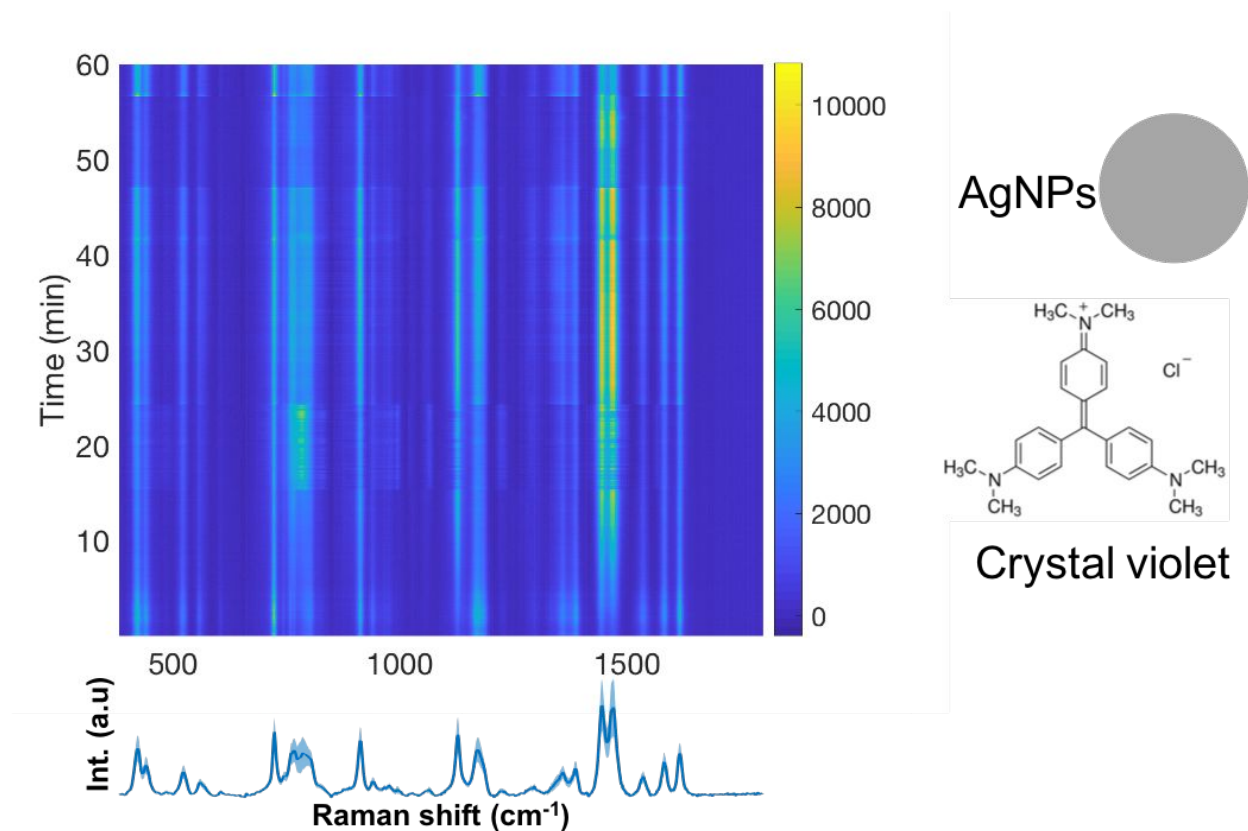

Figure S2: SERS of crystal violet acquired in an extended 60 minutes time frame. The heatmap (RSD=25.0%, n=1800) of 200 nM crystal violet was displayed in pseudocolors reflecting the Raman intensities as shown in the color bars. The averaged Raman spectra were aligned at the bottom with the shaded region indicating the signal variations.

Figure S3: Effect of salt species on SERS detection of fentanyl. Averaged SERS spectra (n=80 for each salt species) acquired by mixing different salt solutions (1 M for NaCl, NaBr, NaI, KCl, KBr, KI and 0.5 M for Na_2SO_4) with AgNPs colloids (Abs. at 409 nm, ~0.6) and fentanyl (200 ng/mL). SERS spectra were offset for clarity.
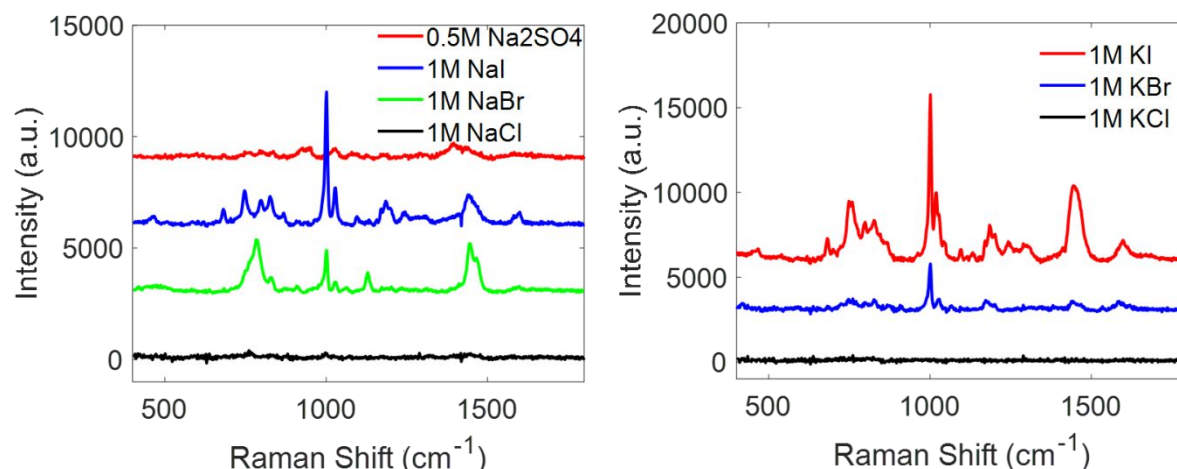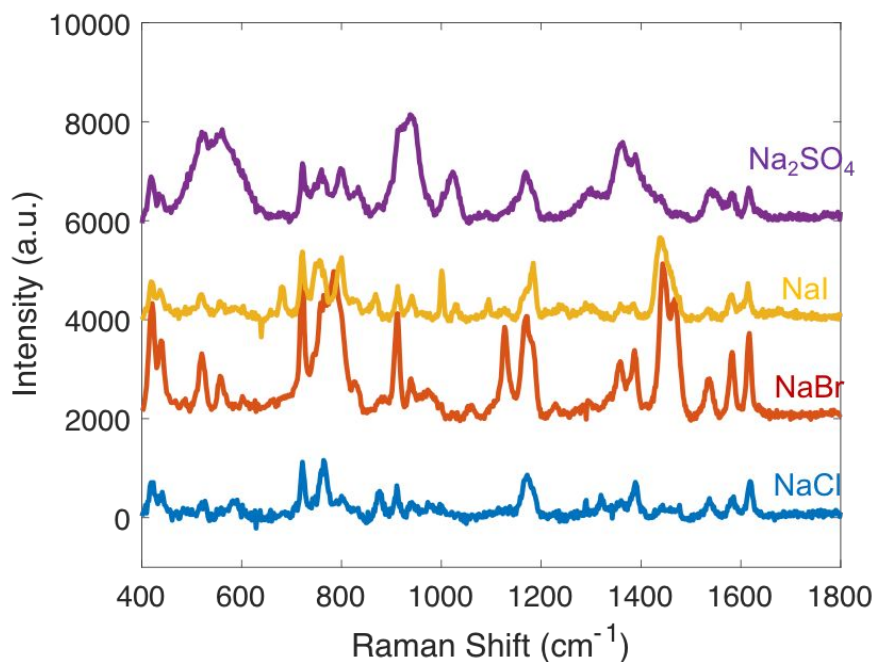

Figure S4: Effect of salt species on SERS detection of crystal violet. Averaged SERS spectra (n=40 for each salt species) acquired by mixing different salt solutions (1 M for NaCl, NaBr, NaI and 0.5 M for Na_2SO_4) with AgNPs colloids (Abs. at 409 nm, ~0.6) and crystal violet (100 nM). SERS spectra were offset for clarity.
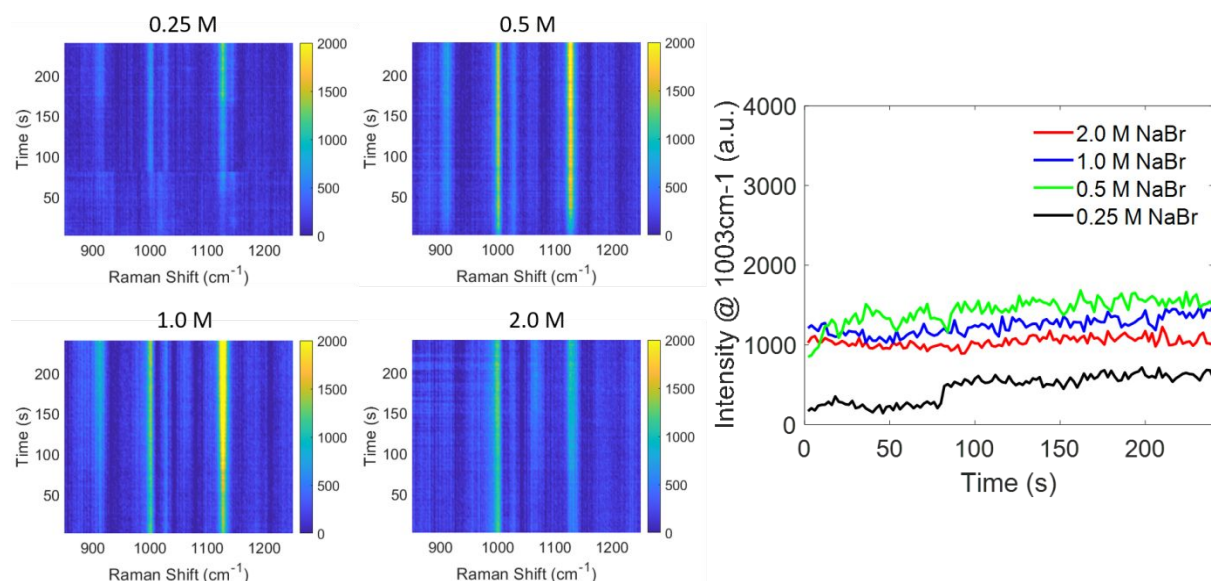
Figure S5. Effect of salt concentration on SERS detection of fentanyl. Time-dependent SERS spectra (n=120) were acquired by adding NaBr of varying concentrations (black: 0.25 M; green: 0.5 M; blue: 1 M; red: 2 M) into the mixture of AgNP colloids and fentanyl. Right panel: temporal evolution of the peak intensity at 1003 cm^{-1}.
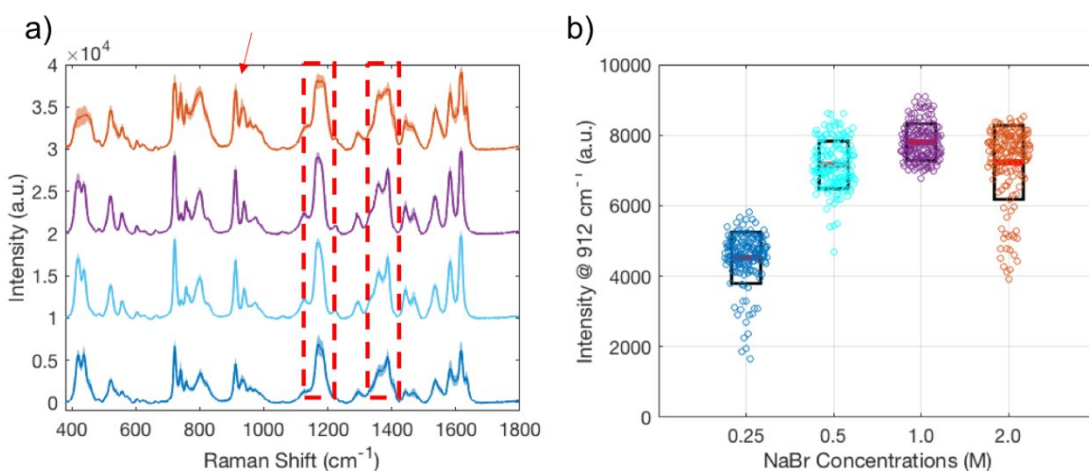
Figure S6. Effect of salt concentration on SERS detection of crystal violet. a) Averaged SERS spectra (n=160) acquired by varying the NaBr salt concentration (blue: 0.25 M; cyan: 0.5 M; purple: 1 M; orange: 2 M) added into the mixture of AgNP colloids and crystal violet. Spectra were offset for clarity and the shaded regions of the spectra represent one standard deviation (1 σ) of the signal across the spectrum and the red arrow indicates the signature Raman peak (912 cm^{-1}) used for peak analysis. B) Fitted peak intensities of the 912 cm^{-1} Raman band obtained from each NaBr concentration with the color codes corresponding to those used in a). The red line is the mean of fitted peak intensities; the black box indicates the standard deviation (±1 σ).

Figure S7. SERS signal reproducibility. SERS signal of fentanyl (200 ng/mL) obtained after mixing with 100 μL as-synthesized AgNP colloidal solution (3 separate batches) and 5 μL NaBr salt (1 M).
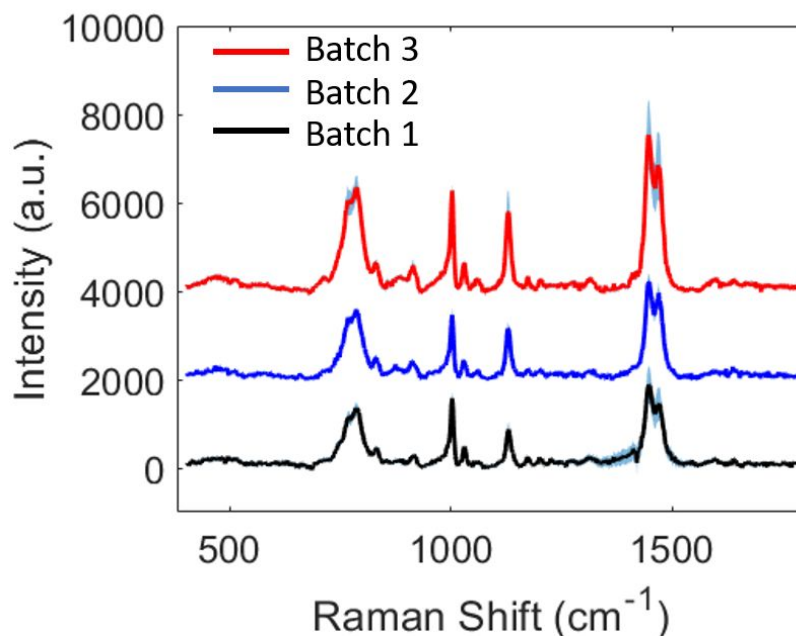

Figure S8: SERS detection of norfentanyl. a) Averaged SERS spectra (n=80 for each concentration) stacked in order of increasing concentrations of the norfentanyl solution (1, 5, 20, 50, 100, 200 μg/mL) from the bottom to the top. The spectra were offset for clarity. The red and black arrows denote the Raman peaks used for quantitative analysis. b) Quantitative analysis using the peak ratio $\frac{I_{(1003\,cm^{-1})}}{I_{(1003\,cm^{-1})} + I_{(1445\,cm^{-1})}}$ between norfentanyl (1003 cm^{-1}) and surface anion residuals (1445 cm^{-1}) plotted against the concentration of norfentanyl. Color codes correspond to those used in a). A Langmuir isotherm (solid red line) was used to fit the data of the entire concentration range and a linear fit was used in the low concentration regime (R^2=0.9421).
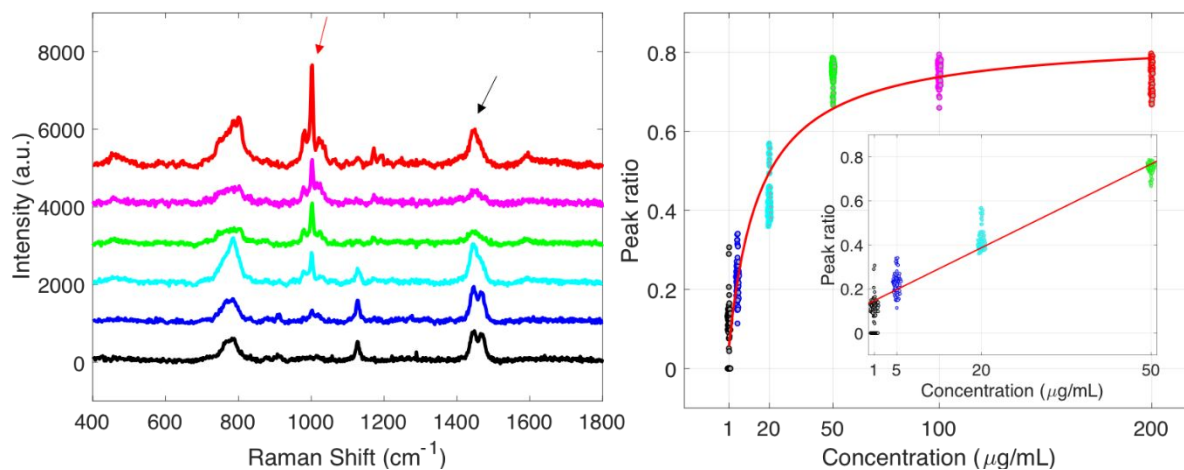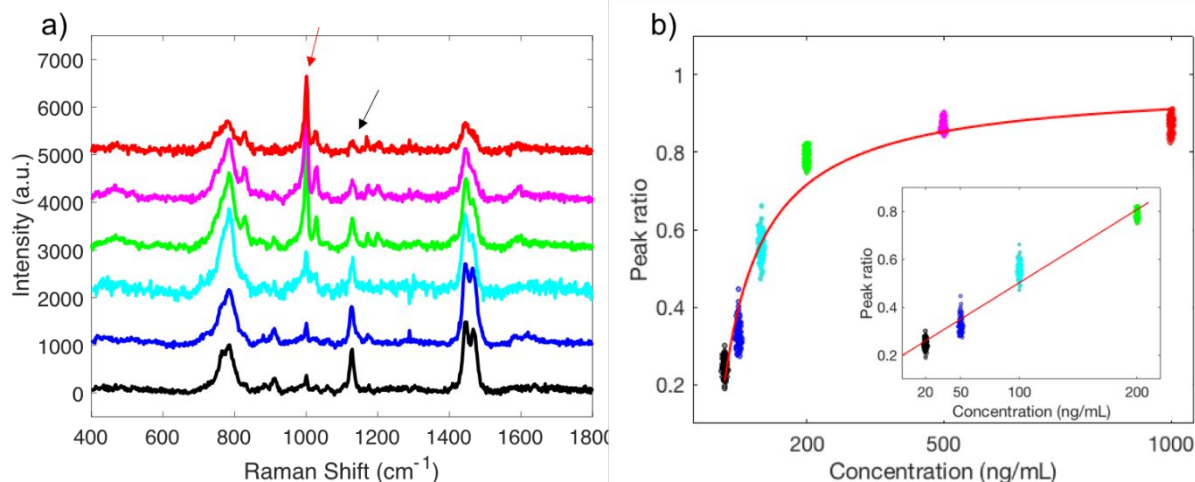
Figure S9: SERS detection of fentanyl. a) Averaged SERS spectra (n=80 for each concentration) stacked in order of increasing concentrations of the fentanyl solution (20, 50, 100, 200, 500, 1000 ng/mL) from the bottom to the top. The spectra were offset for clarity. The red and black arrows denote the Raman peaks used for quantitative analysis. b) Quantitative analysis using the peak ratio $\frac{I_{(1001\,cm^{-1})}}{I_{(1001\,cm^{-1})} + I_{(1127\,cm^{-1})}}$ between fentanyl (1001 cm^{-1}) and surface anion residuals (1127 cm^{-1}) plotted against the concentration of fentanyl. Color codes correspond to those used in a). A Langmuir isotherm (solid red line) was used to fit the data of the entire concentration range and a linear fit was used in the low concentration regime (R^2=0.9600).

Figure S10: Estimation of the limit of detection in fentanyl detection. Averaged SERS spectra (n=80 for each concentration) stacked in the order of increasing concentrations of fentanyl spiked in negative urine control (0, 5, 10, 20, 50, 100, 200, 500, 1000 ng/mL). The blue triangles were peaks attributed to fentanyl and black circles attributed to surface anions. The spectra were offset for clarity. The calculated S/N is ~4.

Figure S11: Quantitative SERS detection of fentanyl mixed in morphine. a) Averaged SERS spectra (n=80) stacked in order of increasing mass concentrations of fentanyl mixed in morphine. b) Quantitative peak analysis using the peak ratios between fentanyl (1001 cm^{-1}) and anionic residues (1127 cm^{-1}) with the same color codes as those in (a). A Langmuir isotherm (solid red line) was used to fit the entire data range and a linear fit used in the low concentration regime (R^2=0.8870).
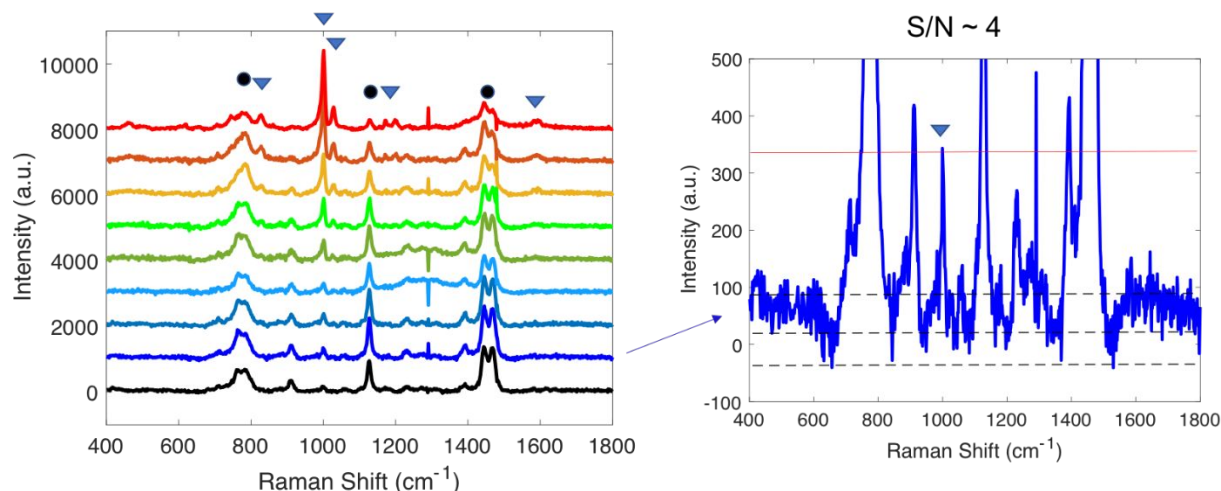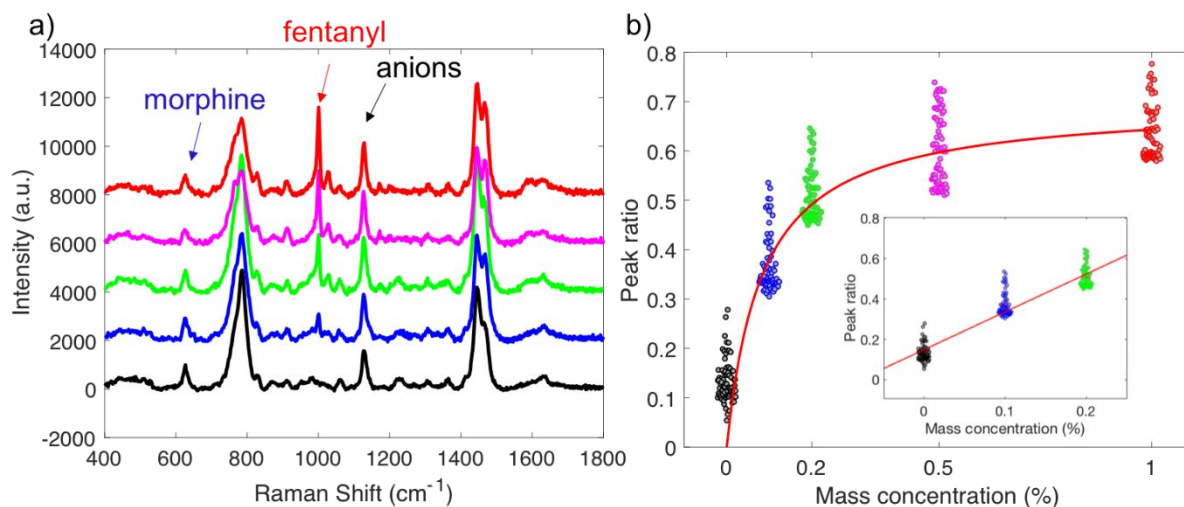

Figure S12: Quantitative SERS detection of fentanyl mixed in oxycodone. a) Averaged SERS spectra (n=80) stacked in order of increasing mass concentrations of fentanyl mixed in oxycodone. b) Quantitative peak analysis using the peak ratios between fentanyl (1001 cm^{-1}) and anionic residues (1127 cm^{-1}) with the same color codes as those in (a). A Langmuir isotherm (solid red line) was used to fit the entire data range and a linear fit used in the low concentration regime (R^2=0.9913).
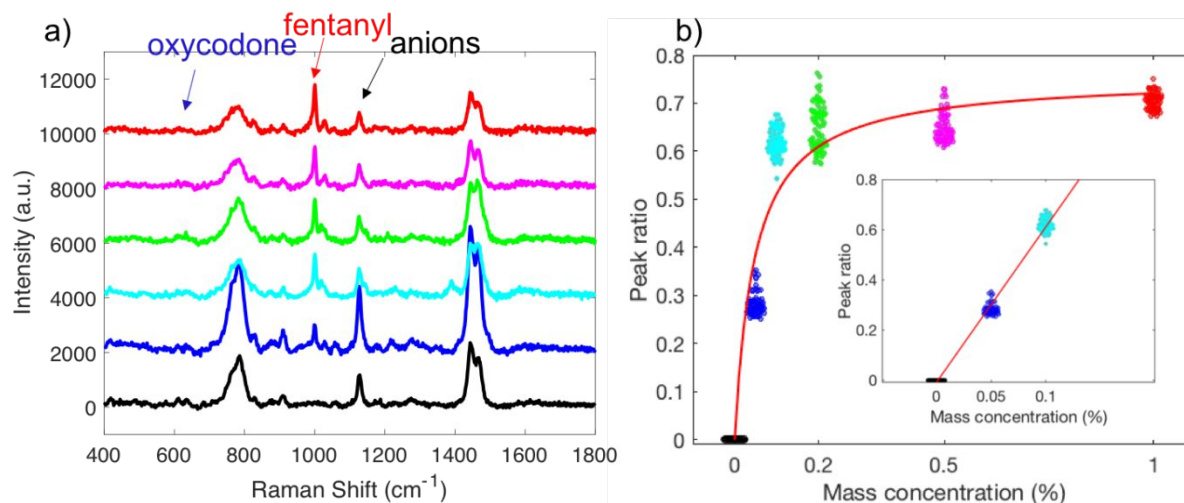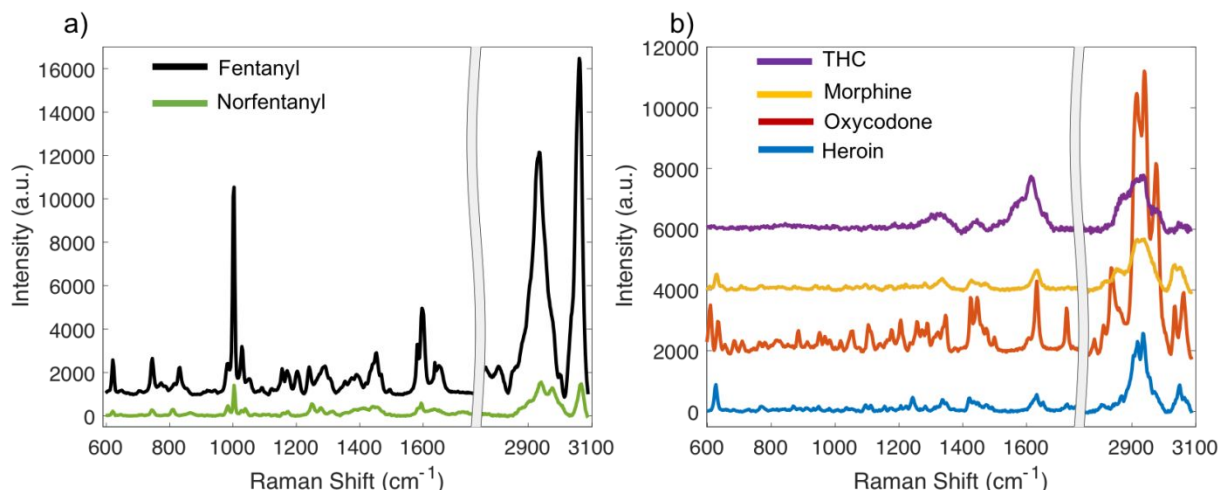
Figure S13: Reference normal Raman spectra for different drug molecules. a) Normal Raman spectra of fentanyl and norfentanyl; b) Normal Raman spectra of THC, morphine, oxycodone, and heroin. Raman spectra were offset for better comparison.
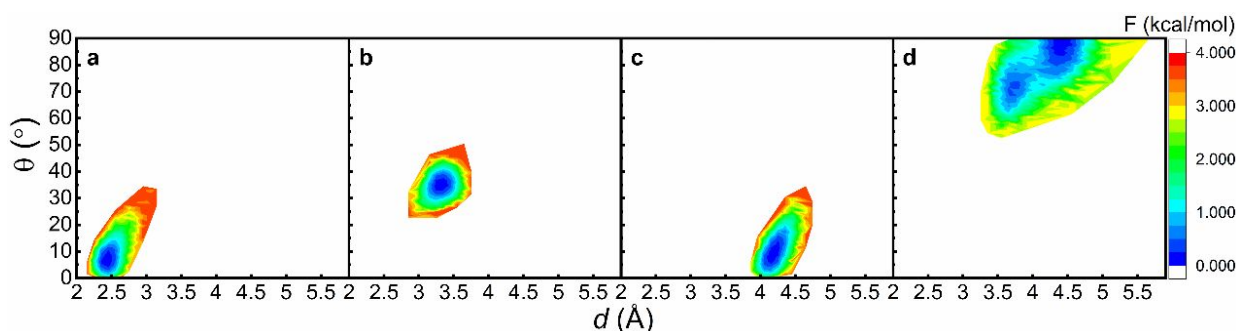

Figure S14: Free energy surfaces for the adsorption of drug molecules on the silver surface. (a) fentanyl, (b) heroin, (c) THC, and (d) protonated norfentanyl. The axes are the distances and angles of the phenyl rings of the drug molecules relative to the silver surface. The free energies are shifted such that the lowest energy is 0.

From Fig. 5, the phenyl rings play an essential role in the adsorption of the drug molecules to the silver surface. We thus calculated the two-dimensional free energy surfaces for the molecular adsorption using the distances and angles from the corresponding phenyl rings to the silver surface. Here for each molecule, we obtained the distance from the geometric center of its phenyl ring, d, and the angle between the surface normal of the phenyl ring and silver surface, θ, and calculated the probability of finding a system with a particular d and θ, P(d,θ). We then computed the free energies as:

$$F = -k_B T ln P(d,\theta) \quad \text{(S1)}$$

Here k_B is Boltzmann constant and T is the simulation temperature. Note that fentanyl contained two phenyl rings and we chose the ring with the C atoms 11-16 (Fig. 5). The resulting free energy surfaces are shown in Figure S14.

From Fig. S14, the phenyl ring in fentanyl (indexes 11-16 of the molecule) adsorbs much closer to the surface than those in THC, heroin, and norfentanyl, consistent with the distance analysis in Fig. 5. In the free energy minimum, the aromatic ring in fentanyl has a distance of 2.4 Å and 7.5° relative to the surface, whereas the distance and angle are 4.2 Å and 7.5o for THC and 3.4 Å and 35.5° for heroin. The phenyl ring in norfentanyl has the largest distance of 4.4 Å and a wider angle-distribution, with the most probable angle at a large value of 89.5°. This suggests that the phenyl ring of norfentanyl barely adsorbs on the silver surface, consistent with the observations in Fig. 5d and h. From Fig. S14, the aromatic-metal interactions are most favorable for fentanyl because its phenyl ring is closest and most parallel to the surface. In comparison, the methyl groups in THC prevent its strong adsorption, allowing its phenyl ring to rotate more freely in space. For heroin, its bent structure (Fig. 5c) causes a much larger angle between its aromatic ring and the surface, weakening its adsorption. Similarly, the bent geometry of norfentanyl (Fig. 5d) pushes its aromatic ring away from the surface with a nearly perpendicular arrangement with respect to the silver surface. As a result, the adsorption of norfentanyl mainly comes from the electrostatic and charge transfer interactions.
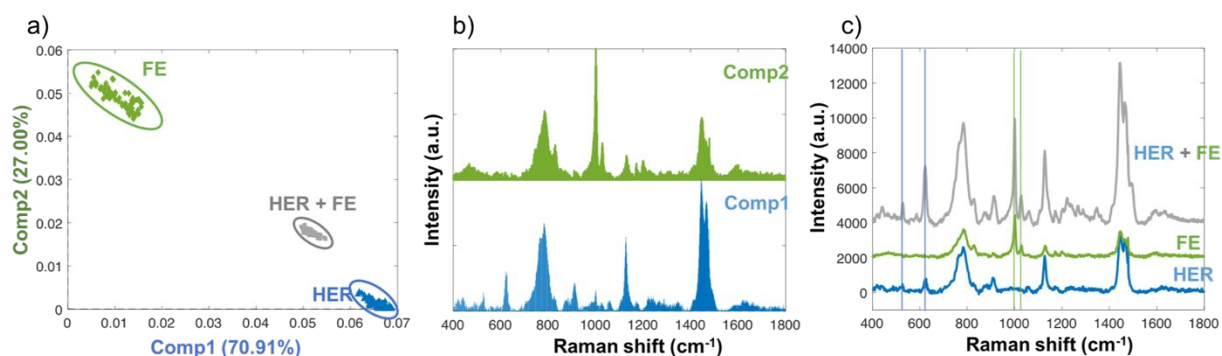

Figure S15: SERS identification of binary mixtures of fentanyl and heroin. a) MCR model-generated 2-D scores plot for Raman signals from individual pure components and the binary mixture (FE: 1 µg/mL; HER: 1 mg/mL); b) pure component spectra as computed from the MCR model with color codes corresponding to those in a); c) Averaged SERS spectra (n=80) from individual pure components with the one from the binary mixture overlaid at the top. Colored regions and guidelines were for peak alignment and assignment.

Figure S16: SERS identification of binary mixtures of fentanyl and oxycodone. a) MCR model-generated 2-D scores plot for Raman signals from individual pure components and the binary mixture (FE: 1 µg/mL; OXY: 1 mg/mL); b) pure component spectra as computed from the MCR model with color codes corresponding to those in a); c) Averaged SERS spectra (n=80) from individual pure components with the one from the binary mixture overlaid at the top. Colored regions and guidelines were for peak alignment and assignment.
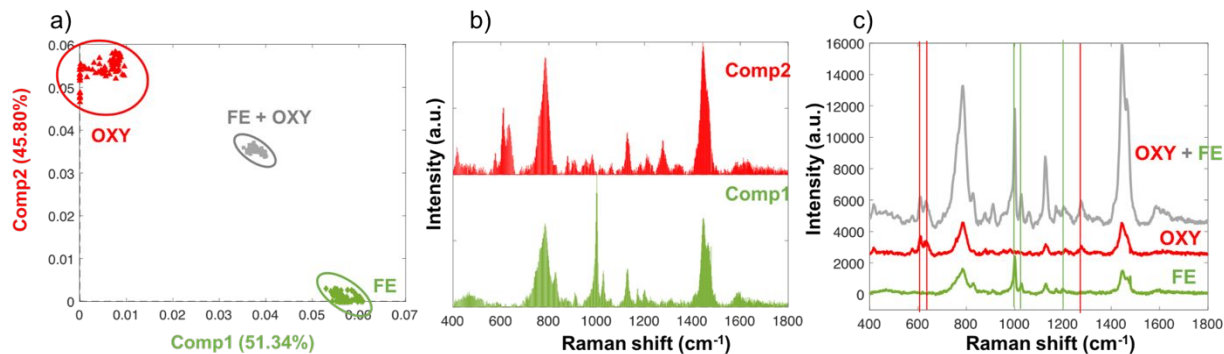

Figure S17: SERS identification of binary mixtures of oxycodone and heroin. a) MCR model-generated 2-D scores plot for Raman signals from individual pure components and the binary mixture (OXY: 1 mg/mL; HER: 1 mg/mL); b) pure component spectra as computed from the MCR model with color codes corresponding to those in a); c) Averaged SERS spectra (n=80) from individual pure components with the one from the binary mixture overlaid at the top. Colored regions and guidelines were for peak alignment and assignment.
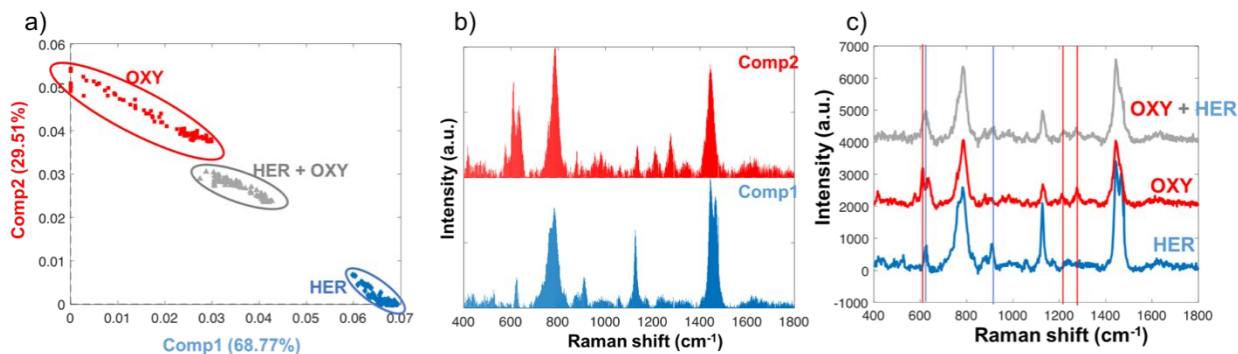
Table S1: SERS signal variations characterized by STD & % RSD in Fig. 3&4

% RSD for Fig. 3b			% RSD for Fig. 4b			% RSD for Fig. 4d		
Concentration (ng/mL)	STD	% RSD	Mass concentration (%)	STD	% RSD	Mass concentration (%)	STD	% RSD
0	0.01	9.87	0.05	0.02	13.78	0.1	0.06	28.16
5	0.02	9.08						
10	0.01	6.28	0.1	0.01	6.19	0.2	0.06	21.06
20	0.03	10.45						
50	0.03	9.29	0.2	0.02	4.18	0.5	0.05	11.72
100	0.06	11.71				1	0.02	3.51
200	0.04	7.07	0.5	0.02	3.03			
500	0.04	4.92				2	0.04	6.78
1000	0.02	2.15	1	0.02	3.88	5	0.02	2.52